Phys. Status Solidi B **254**, No. 5, 1600800 (2017) / **DOI** 10.1002/pssb.201600800

physica status solidi b
www.pss-b.com
basic solid state physics

Unpinning of heavy hole spin in magnetic quantum dots

I. V. Dinu[1], V. Moldoveanu[*,1], R. Dragomir[1], and B. Tanatar[2]

[1] National Institute of Materials Physics, PO Box MG-7, Bucharest-Magurele, Romania
[2] Department of Physics, Bilkent University, Bilkent, 06800 Ankara, Turkey

Received 14 November 2016, revised 24 November 2016, accepted 2 December 2016
Published online 30 December 2016

Keywords CdTe, dynamics, excitons, Kohn–Luttinger theory, magnetic quantum dots, manganese

[*] Corresponding author: e-mail valim@infim.ro, Phone: +40-(0)21-3690185, Fax: +40-(0)21-3690177

Using the $k \cdot p$ theory and configuration interaction method, we analyze the effect of heavy hole–light hole (HH–LH) mixing in CdTe quantum dots (QDs) with a single manganese (Mn) ion. We find that the hole-Mn exchange switches the coupling between two excitons whose Luttinger spinors have both HH and LH components. If the magnetic dopant is off-centered and the QD is subjected to a single π pulse the system periodically bounces between bright and dark mostly HH excitons with opposite HH spins. A pump-and-probe setup allows to estimate the efficiency of this HH spin unpinning from the biexciton response. The biexciton absorption spectrum is also discussed.

1 Introduction The valence-band (VB) mixing in self-assembled quantum dots is due to spin-orbit coupling and depends either on the QD aspect ratio [1] or on strain [2]. The $k \cdot p$ calculations show that by increasing the aspect ratio the VB Luttinger spinors develop minor and dominant LH or HH components. Although this HH–LH mixing emerges at the level of single-particle hole states, it must leave its fingerprint on the spectral or optical properties. Indeed, Siebert et al. [3] argued that the HH–LH coupling induces the zero-field splitting within the p-shell hole states. Later on, Climente [4] discussed the role of the HH–LH coupling on the two-hole triplet splitting and on the spin purity of charged trions in InAs/GaAs QDs.

In this Letter, we theoretically investigate the HH–LH mixing effects in optically active QD with an embedded magnetic impurity, that is, a Mn atom. The extensive experimental [5] and theoretical work on this system mainly aim to manipulate the Mn spin ($M = 5/2$) via its exchange interaction with electrons and holes [6]. It has been proposed that the electron-Mn exchange interaction can be used to prepare a dark HH exciton and to completely flip the Mn spin [7, 8]. These protocols assume, however, purely HH or purely LH states. We recall that HH band-edge Bloch states are $|J_z = \pm 3/2\rangle$ such that the hole spin cannot be reversed by changing the Mn spin by $\Delta M_z = \pm 1$. Nonetheless, when LH states $|J_z = \pm 1/2\rangle$ come into play the so called HH spin pinning can be removed due to intermediate transitions $J_z = \pm 3/2 \rightarrow J_z = \pm 1/2$. To our best knowledge, the combined effects of HH–LH mixing and hole-Mn exchange in single-Mn QD are still poorly studied. However Goryca et al. studied the brightening of the dark exciton due to valence band mixing [9]. Also, in a recent work Varghese et al. [10] measured the dynamics of a single hole which is exchange-coupled to a Mn spin embedded in a QD. They have found that the VB mixing leads to hole-Mn spin relaxation. In a previous work, we have also studied the dynamics of mostly LH excitons and mixed biexcitons in single-Mn doped QDs [11].

Here, we predict that the interplay between the HH–LH mixing and the hole-Mn exchange interaction induces a coupling between a dominant HH $J_z = \pm 3/2$ component and the minor LH $J_z = \pm 1/2$ component of two Luttinger spinors belonging to a Kramers doublet. Due to the short-range nature of the exchange interaction, this coupling is given by a non-vanishing overlap of two envelope functions with different azimuthal quantum number m_z at the Mn location. As a consequence, the HH spin underpinning is maximal when the Mn atom is off-centered. We also obtain exchange-induced Rabi (EXR) oscillations of the populations corresponding to a bright HH spin-up and spin-down dark exciton populations. The model and theoretical tools are summarized in Section 2 (for more details see Ref. [11]). In Section 3, we present and discuss the results, while Section 4 is left for conclusions.

2 The model We consider cylindrical QDs of radius R and height W. The single particle states are obtained by diagonalizing the $k \cdot p$ Hamiltonian $H_{kp} = H_C + H_{KL}$, where H_C describes the electrons in the conduction band (CB) and H_{KL} is the Kohn–Luttinger Hamiltonian for holes. A Luttinger spinor state for which $H_{kp}|F_z, i\rangle = E_i^h|F_z, i\rangle$ reads as [12]:

$$|F_z, i\rangle = \sum_{n,l} \begin{pmatrix} C^{F_z,i}_{\frac{3}{2},n,l}|\phi_{(F_z-\frac{3}{2})nl}, \Uparrow_H\rangle \\ C^{F_z,i}_{-\frac{1}{2},n,l}|\phi_{(F_z+\frac{1}{2})nl}, \Downarrow_L\rangle \\ C^{F_z,i}_{\frac{1}{2},n,l}|\phi_{(F_z-\frac{1}{2})nl}, \Uparrow_L\rangle \\ C^{F_z,i}_{-\frac{3}{2},n,l}|\phi_{(F_z+\frac{3}{2})nl}, \Downarrow_H\rangle \end{pmatrix}, \quad (1)$$

where the double arrows stand for LH or HH spin and the weights of various J_z components with envelope functions $\phi_{m_z nl}$ are given by $|C^{F_z}_{J_z,n,l}|^2$. Each Luttinger spinor has a well defined total orbital quantum number $F_z = J_z + m_z$. The envelopes $\phi_{m_z nl}$ are built from Bessel functions J_{m_z} and eigenfunctions ξ_l associated to the vertical confinement ($\alpha_n^{m_z}$ is the n-th zero of the Bessel function):

$$\phi_{m_z nl}(\rho, \theta, z) = \frac{e^{im_z\theta}}{\sqrt{\pi}R} \frac{J_{m_z}(\alpha_n^{m_z}\rho/R)}{|J_{m_z+1}(\alpha_n^{m_z})|} \xi_l(z). \quad (2)$$

The single-electron states in the CB are denoted by $|S_z, j\rangle$, where S_z denotes the electron spin. The exchange interaction between the electron (hole) spins $\hat{\mathbf{S}}$ ($\hat{\mathbf{J}}$) and the Mn spin $\hat{\mathbf{M}}$ located at $\mathbf{R}_{Mn}$ is given by:

$$\begin{aligned} H_X &= -J_e\hat{\mathbf{S}}\cdot\hat{\mathbf{M}}\delta(\mathbf{r}_e - \mathbf{R}_{Mn}) + J_h\hat{\mathbf{J}}\cdot\hat{\mathbf{M}}\delta(\mathbf{r}_h - \mathbf{R}_{Mn}) \\ &= H_{e-Mn} + H_{h-Mn}, \end{aligned} \quad (3)$$

J_e and J_h are the corresponding exchange interaction strengths. In the absence of the Mn-QD exchange interaction, one uses the configuration interaction method to calculate "exchange-free" exciton and biexciton states $|\nu, M_z\rangle$ defined by the equation $\hat{H}_0|\nu, M_z\rangle = \mathcal{E}_\nu|\nu, M_z\rangle$ where $\hat{H}_0 = \hat{H}_{KL} + \hat{H}_C + \hat{H}_{coul} + D_0\hat{M}_z^2$, and the hat denotes the second quantized form of the single-particle operators. The diagonalization implies all many-body configurations generated by the highest energy N_V single-particle states in the VB and by the lowest energy N_C states in the CB (more details are given in [11]). $\hat{H}_{coul}$ describes the Coulomb interaction. $D_0\hat{M}_z^2$ is a small contribution due to magnetic anisotropy [10].

When written with respect to states $|\nu, M_z\rangle$ the exchange interaction $\hat{H}_{h-Mn}$ contains a diagonal Ising term arising from $\hat{J}_z\hat{M}_z$ and spin-flip terms from $\hat{J}_\pm\hat{M}_\mp$:

$$\begin{aligned} \langle\nu, M_z|\hat{H}_{h-Mn}|\nu', M_z'\rangle &= J_h\sum_{i,j=1}^{N_V}\overline{\psi_i^h}(\mathbf{R}_{Mn})\psi_j^h(\mathbf{R}_{Mn}) \\ &\times\langle J_z^i M_z|\hat{J}_\pm\hat{M}_\mp|J_z^j M_z'\rangle\langle\nu|b_i^\dagger b_j|\nu'\rangle, \end{aligned} \quad (4)$$

where $b_i^\dagger(b_i)$ create (annihilate) the single-particle hole state $\psi_i^h(\mathbf{r}) := \langle\mathbf{r}|F_z, i\rangle$. From Eq. (4), it follows that the exchange-induced coupling between the two Luttinger spinors depends not only on the weights of the LH and HH components but also on the "overlap" $\overline{\phi}_{m_z nl}\phi_{m_z' n' l'}$ of envelope functions at the Mn location $\mathbf{R}_{Mn}$. In the case of electron-Mn exchange interaction such an analysis has been presented in [13].

We then solve the Liouville–von Neumann (LvN) equation $i\hbar\dot{\hat{\rho}}(t) = [\hat{H}_0 + \hat{H}_X + \hat{V}_R(t), \hat{\rho}(t)]$ for the density operator $\hat{\rho}$ in the basis $\{|\nu, M_z\rangle\}$, where $\hat{V}_R(t)$ describes the light-matter interaction which is treated clasically. We shall denote by $P_{\nu,M_z} := \langle\nu, M_z|\hat{\rho}(t)|\nu, M_z\rangle$ the population of the state $|\nu, M_z\rangle$. Fore more details we refer to [11].

3 Results and discussion We present results for a QD of radius $R = 5$ nm and height $W = 8$ nm. The aspect ratio $W/2R$ controls the HH–LH mixing within a Luttinger spinor [4]. Typically, one has a single dominant component $|\phi_{m_z nl}, J_z\rangle$ and some minor components. We shall focus on the highest energy Kramers doublet in the VB which corresponds to $F_z = \pm 3/2$. The next doublet corresponds to mostly LH spinors and lies 9 meV below the HH doublet. The dominant components (around 90% weight) of the Luttinger spinors are HHs while the minor components (up to 5% weight each) are LH-like. The Mn location $\mathbf{R}_{Mn}$ is specified by its cylindrical coordinates $\rho_{Mn}, \theta_{Mn}, z_{Mn}$. $\rho_{Mn} = z_{Mn} = 0$ define the QD center.

The exciton states $|\nu, M_z\rangle$ are labeled by their total spin $S_z + F_z$ and we have two bright $|B \pm 1, M_z\rangle$ and two dark states $|D \pm 2, M_z\rangle$. The electron-hole short-range exchange induces a splitting between the bright and dark [14] excitons $\delta = 0.46$ meV. The two exchange coupling strengths in CdTe are $J_e = 15\text{eV}\text{Å}^3$ and $J_h = 60\text{eV}\text{Å}^3$. We fix $D_0 = 12\mu\text{eV}$.

We begin our analysis by describing how the hole-Mn exchange-interaction combines with the HH–LH mixing to couple a pair of bright and dark excitons with opposite HH spin. Let us consider the bright exciton $|B - 1, 5/2\rangle$. The four largest weight components of the associated Luttinger spinor $F_z = -3/2$ are: ($|\phi_{-312}, \Uparrow_H\rangle$, $|\phi_{-112}, \Downarrow_L\rangle$, $|\phi_{-211}, \Uparrow_L\rangle$, $|\phi_{011}, \Downarrow_H\rangle$). On the other hand, the dark exciton $|D + 2, 3/2\rangle$ contains ($|\phi_{011}, \Uparrow_H\rangle$, $|\phi_{211}, \Downarrow_L\rangle$, $|\phi_{112}, \Uparrow_L\rangle$, $|\phi_{312}, \Downarrow_H\rangle$) as components of $|F_z = 3/2\rangle$. Then from Eq. (4), we infer that the dominant HH component of each exciton is exchange-coupled to one LH minor component of the other one. The relevant envelope overlaps leading to this coupling are $\phi_{011}\phi_{211}$ and $\phi_{011}\phi_{-211}$. Smaller contributions are associated either to different zeros of the Bessel function or to different quantum numbers l.

In Fig. 1a, we show the bright-dark HH exciton coupling $v_{HH} = \langle D + 2, 3/2|\hat{H}_X|B - 1, 5/2\rangle$ as a function of the radial coordinate of the Mn atom ρ_{Mn}. It displays a

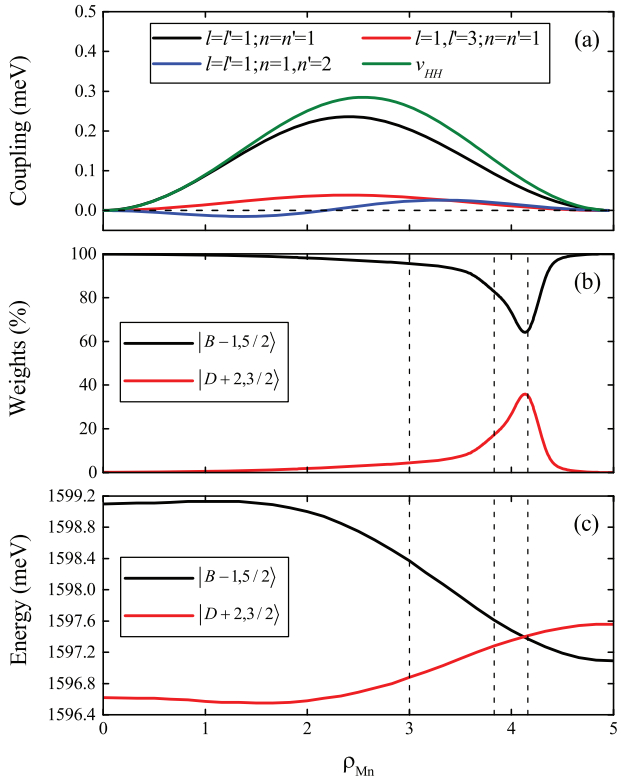

Figure 1 (a) The contributions of diferrent envelope function overlaps $\bar{\phi}_{m_z nl}(\mathbf{R}_{\rm Mn})\phi_{m_z' n' l'}(\mathbf{R}_{\rm Mn})$ to the coupling $v_{\rm HH}$ between the bright and dark HH excitons as function of $\rho_{\rm Mn}$. Each overlap obeys the condition $m_z - m_z' = 2$. (b) The weights of exciton states $|D+2,3/2\rangle$ and $|B-1,5/2\rangle$ in a fully interacting exciton state as a function $\rho_{\rm Mn}$. (c) The HH exciton levels in the absence of spin-flip processes. For simplicity we fixed $\theta_{\rm Mn} = z_{\rm Mn} = 0$. The vertical lines mark specific values of $\rho_{\rm Mn}$ which will be used when further discussing our results.

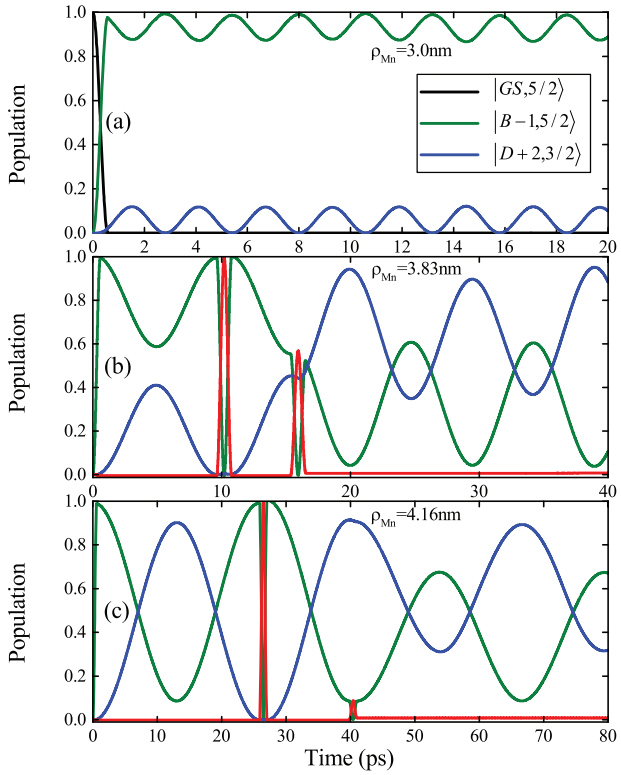

Figure 2 The populations of bright and dark HH excitons as functions of $\rho_{\rm Mn}$. The bright exciton is created by a σ_- π pulse. (a) $\rho_{\rm Mn} = 3$ nm. (b) $\rho_{\rm Mn} = 3.83$ nm, (c) $\rho_{\rm Mn} = 4.16$ nm. The red line in Figs. (b) and (c) shows the biexciton response to two σ_+ probe pulses.

maximum at $\rho_{\rm Mn} = 2.6$ nm and vanishes both at the origin and on the cylinder edge $\rho_{\rm Mn} = 5$ nm. This behavior emerges from the overlap of various envelope functions which compose the Luttinger spinors $|F_z = \pm 3/2\rangle$. Both overlaps vanish at the origin because $J_2(0) = 0$.

By looking at Fig. 1a, one would expect a strong mixing between the bright and dark excitons around $\rho_{\rm Mn} = 2.6$ nm where the coupling $v_{\rm HH}$ is maximum. However, the weights of the exchange-free HH excitons within a fully interacting state (see Fig. 1b) show that as long as $\rho_{\rm Mn} < 2$ nm the mixing is negligible and reaches a maximum value around $\rho_{\rm Mn} = 4.12$ nm. To understand this result we give in Fig. 1c the bright and dark excitons levels calculated in the absence of the spin-flip terms. In this case the level spacing is given by the bright-dark exciton splitting δ and the Ising shift from the hole-Mn and electron-Mn interaction. The largest gap corresponds to $\rho_{\rm Mn} = 0$ and as long as $\rho_{\rm Mn} < 3.75$ nm exceeds by far the coupling term $v_{\rm HH}$. The strongest mixing coincides with the degeneracy point between the exciton levels. At $\rho_{\rm Mn} = 5$ nm one recovers the bright-dark exciton splitting δ.

To investigate the effect of the Mn-mediated coupling $v_{\rm HH}$ on exciton dynamics we use a setup similar to the one proposed in Ref. [8]. In Fig. 2a, the bright exciton $|B-1,5/2\rangle$ is optically addressed by an ultrafast σ_- pulse. The initial ground state $|{\rm GS}, M_z = 5/2\rangle$ corresponds to a fully occupied VB and empty CB [15]. When the exciton population reaches a maximum (i.e., after a π rotation on the Bloch sphere) the pulse stops and the system dynamics is entirely controlled by the exciton-Mn exchange interaction. Note that $\langle D+2,3/2|\hat{S}_\pm \hat{M}_\mp|B-1,5/2\rangle = 0$ since $S_z = 1/2$ and $M_z = 5/2$ and, therefore, the effect of the electron-Mn exchange reduces to an Ising shift. Then if the heavy-hole pinning holds the system should indefinitely remain in the bright exciton state. We find that this is true for $\rho_{\rm Mn} < 2$ nm (not shown). However, as $\rho_{\rm Mn}$ increases further the excitonic populations shown in Fig. 2 display periodic oscillations. First, we notice small amplitude EXR oscillations at $\rho_{\rm Mn} = 3$ nm. Then the oscillation amplitude increases considerably for $\rho_{\rm Mn} = 3.83$ nm and almost reaches its maximum value at $\rho_{\rm Mn} = 4.16$ nm.

The emergence of clear EXR oscillations at some locations of the Mn atom coincides with non-vanishing overlaps of the LH and HH components of Luttinger spinors $|F_z = \pm 3/2\rangle$ shown in Fig. 1a and with the stronger or weaker mixing between the two HH excitons in Fig. 1b. As

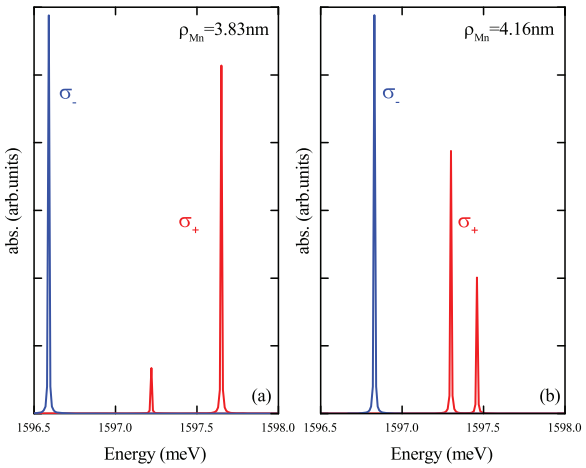

Figure 3 The *s*-shell biexcionic absorption spectrum for two values of the Mn location. (a) $\rho_{\mathrm{Mn}} = 3.83$ nm, (b) $\rho_{\mathrm{Mn}} = 4.16$ nm.

expected, the period and amplitude of the EXR oscillations are controlled by the gap shown in Fig. 1c. In particular, a fast switching (around 27 ps) of the dominant HH component is achieved in Fig. 2c.

In Fig. 2b and c, we simulate a pump-and-probe setting which allows one to estimate the degree of mixing between the two excitons for a given ρ_{Mn}. The pump signal is the same as in Fig. 2a and the probe signal is a σ_+ 2π pulse whose frequency roughly matches the transition from the bright exciton to the *s*-shell HH biexciton. It is clear that if the probe pulse coincides with a maximum/minimum of the bright exciton population the biexciton response is strong/weak. The resulting sequence of maxima and minima could be used to confirm the existence of the exchange-induced coupling between the bright and dark HH exciton. Note that after the 2nd probe pulse the Rabi oscillation changes its slope. This happens because the coherence $\langle B-1, 5/2|\hat{\rho}|D+2, 3/2\rangle$ undergoes a phase shift (see the discussion in [7]). The proposed pump-and-probe setup is not affected by intraband relaxation processes as we deal with *s*-shell excitons and biexcitons.

Finally, we point out that the bright and dark HH mixing changes the PL spectrum associated to the ground state HH biexciton. Indeed, each of the fully interacting states contain a "bright" component from $|B-1, 5/2\rangle$ and, therefore, a σ_+ pulse leads to two biexciton peaks. This feature is confirmed in Fig. 3. On the contrary, if the system is in the state $|B+1, 5/2\rangle$ a single biexciton signal appears when a σ_- pulse is applied. This happens because $|B+1, 5/2\rangle$ is not mixed by the Mn-exchange: on one hand, the electron-Mn coupling almost vanishes away from QD center and on the other hand, hole-Mn spin flipping is forbidden by selection rules. A similar pattern appears in the exciton absorption spectrum associated to a σ_- pulse. Note that in order to recover the well known six lines spectrum one has to consider all values of the Mn spin. Here, we considered that the initial state corresponds to a single value $M_z = 5/2$. We found similar results for other parameters of R and W provided the aspect ratio favors the HH–LH mixing. The EXR oscillation should develop at low (few K) temperature typical to experiments on Mn-doped QDs.

4 Conclusions We predict HH–LH mixing effects on the HH exciton structure of single-Mn QDs. It turns out that a pair of bright and dark excitons with opposite HH spins are coupled by the hole-Mn exchange if some of the envelope functions belonging to their Luttinger spinors overlap at the Mn location. Furthermore, we obtain the exchange-induced Rabi oscillations of populations associated to bright and dark HH excitons. One can trace back the magnitude of the HH–LH mixing by looking either at the biexciton absorption spectra either at the EXR oscillations for different values of the Mn radial coordinate.

Acknowledgement V.M, I.V.D., and R.D acknowledge financial support from PNCDI2 program (grant PN-II-ID-PCE-2011-3-0091) and from Romanian Core Research Programme PN16-480101. B.T. acknowledges partial support from TUBITAK (112T619) and TUBA.

References

[1] C. Segarra, J. I. Climente, and J. Planelles, J. Phys.: Condens. Matter **24**, 115801 (2012).
[2] Y. Léger, L. Besombes, L. Maingault, and H. Mariette, Phys. Rev. B **76**, 045331 (2007).
[3] E. Siebert, T. Warming, A. Schliwa, E. Stock, M. Winkelnkemper, S. Rodt, and D. Bimberg, Phys. Rev. B **79**, 205321 (2009).
[4] J. I. Climente, Solid State Commun. **152**, 825 (2012).
[5] L. Besombes, Y. Léger, L. Maingault, D. Ferrand, H. Mariette, and J. Cibert, Phys. Rev. Lett. **93**, 207403 (2004).
[6] J. Fernández-Rossier, Phys. Rev. B **73**, 045301 (2006).
[7] D. E. Reiter, V. M. Axt, and T. Kuhn, Phys. Status Solidi B **246** 779 (2009).
[8] D. E. Reiter, T. Kuhn, and V. M. Axt, Phys. Rev. Lett. **102**, 177403 (2009).
[9] M. Goryca, P. Plochocka, T. Kazimierczuk, P. Wojnar, G. Karczewski, J. A. Gaj, M. Potemski, and P. Kossacki, Phys. Rev. B **82**, 165323 (2010).
[10] B. Varghese, H. Boukari, and L. Besombes, Phys. Rev. B **90**, 115307 (2014).
[11] V. Moldoveanu, I. V. Dinu, R. Dragomir, and B. Tanatar, Phys. Rev. B **93**, 165421 (2016).
[12] J. I. Climente, M. Korkusinski, G. Goldoni, and P. Hawrylak, Phys. Rev. B **78**, 115323 (2008).
[13] F. Qu and P. Hawrylak, Phys. Rev. Lett. **95**, 217206 (2005).
[14] E. Kadantsev and P. Hawrylak, Phys. Rev. B **81**, 045311 (2010).
[15] Such a ground state can be prepared by applying a small magnetic field.